Electronic Supplementary Information(ESI)

High Thermoelectric Performance in Tellurium Free *p*-type $AgSbSe_2$[†]

Satya N. Guin,[a] Arindom Chatterjee,[a] Devendra Singh Negi,[b,c] Ranjan Datta,[b,c] and Kanishka Biswas*[,a]

[a]*New Chemistry Unit,* [b]*Chemistry and Physics of Materials Unit and* [c]*International Centre for Materials Science,*
Jawaharlal Nehru Centre for Advanced Scientific Research (JNCASR),
Jakkur P.O., Bangalore 560064 (India)

**Email: kanishka@jncasr.ac.in*

Experimental Section

Reagents. Elemental Silver (Ag, 99.9%, metal basis), elemental antimony (Sb, 99.9999%, metal basis), elemental bismuth (Bi, 99.999 %), elemental selenium (Se, 99.999%, metal basis), were purchased from Alfa Aesar and used for synthesis without further purification.

Synthesis. Ingots (~9 g) of $AgSb_{1-x}Bi_xSe_2$ (x = 0.02, 0.04), $AgSb_{1-x}Pb_xSe_2$ (x = 0.02, 0.04) and pristine $AgSbSe_2$ were synthesized by mixing appropriate ratios of high-purity starting materials of Ag, Sb, Bi or Pb and Se in quartz tube. The tubes were sealed under high vacuum (~10^{-5} Torr) and slowly heated up to 673 K over 12 h, then heated up to 1123 K in 4h, soaked for 10 h, and subsequently air quenched to room temperature. For electrical and thermal transport measurements the samples were cut and polished. Bar-shaped sample is used for simultaneous electrical conductivity and Seebeck coefficient measurement, whereas coin-shaped sample is used for thermal conductivity measurement.

Powder X-ray diffraction. Powder X-ray diffraction for all the samples were recorded using a Cu K_α (λ = 1.5406 Å) radiation on a Bruker D8 diffractometer.

Band gap measurements. To probe optical energy gap of these compounds, optical diffuse reflectance measurements were performed on finely ground powders at room temperature. The spectra were recorded at the range of 200 nm to 3000 nm using a Perkin Elmer Lambda 900, UV/Vis/NIR spectrometer. Absorption (α/Λ) data were calculated from reflectance data using Kubelka-Munk equations: $\alpha/\Lambda = (1 - R)^2/(2R)$, where R is the reflectance and α and Λ are the absorption and scattering coefficients, respectively. The energy band gaps were derived from α/Λ vs. E (eV) plots. TEM imaging was performed using an aberration corrected FEI TITAN3TM 80-300 keV transmission electron microscope operating at 300 keV.

Electrical properties and carrier concentration: σ and S were measured simultaneously on a sample of the dimension, 2 mm ×3 mm ×8 mm, under a helium atmosphere from 290 K to 723 K by ULVAC-RIKO ZEM-3 instrument. The longer direction of the sample coincides with the direction in which the thermal conductivity was measured. Electrical properties obtained from different slices from the same sample were similar.

Carrier concentrations were determined using Hall coefficient measurements at room temperature with an ECOPIA HMS 3000 system. A four-contact Hall-bar geometry was employed and both negative and positive polarity was applied to estimate Joule resistive errors.

Thermal diffusivity, D , was directly measured and heat capacity, Cp , was indirectly derived using standard sample (pyroceram) in the range 298–723 K by using laser flash diffusivity method in a Netzsch LFA-457. Coins with 8 mm diameter and 2 mm thickness were used in this measurements. κ_{total} was estimated using the formula, $\kappa_{total} = DC_p\rho$, where ρ is the density of the sample, measured from sample dimension and mass. Densities of the samples are ~96 % of the theoretical density. Thermal conductivity was measured in the same direction of the electrical transport measurement.

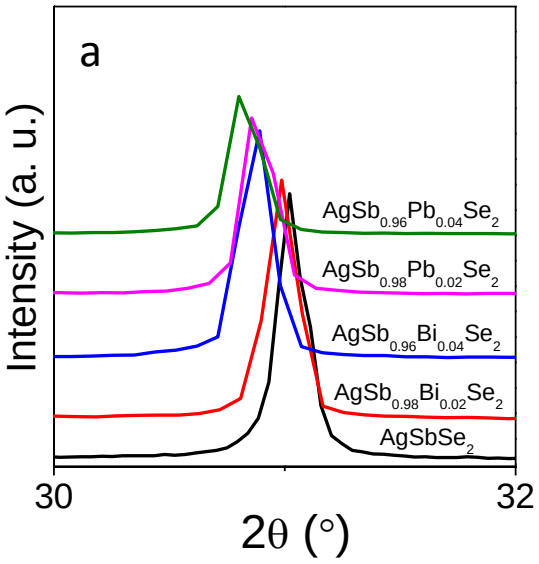

Fig. S1 (a) Lower angle shift of PXRD peak due to incoropration of Bi/ Pb in $AgSbSe_2$.

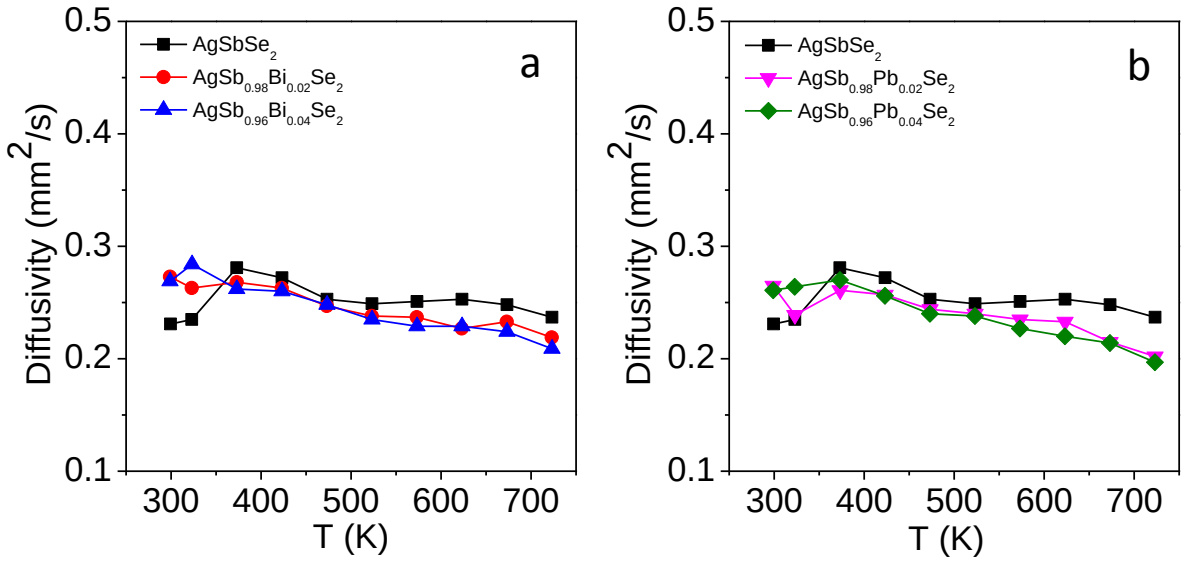

Fig. S2 Temperature dependent thermal diffusivity of (a) $AgSb_{1-x}Bi_xSe_2$ (x= 0-0.04) and (b) $AgSb_{1-x}Pb_xSe_2$ (x= 0- 0.04).

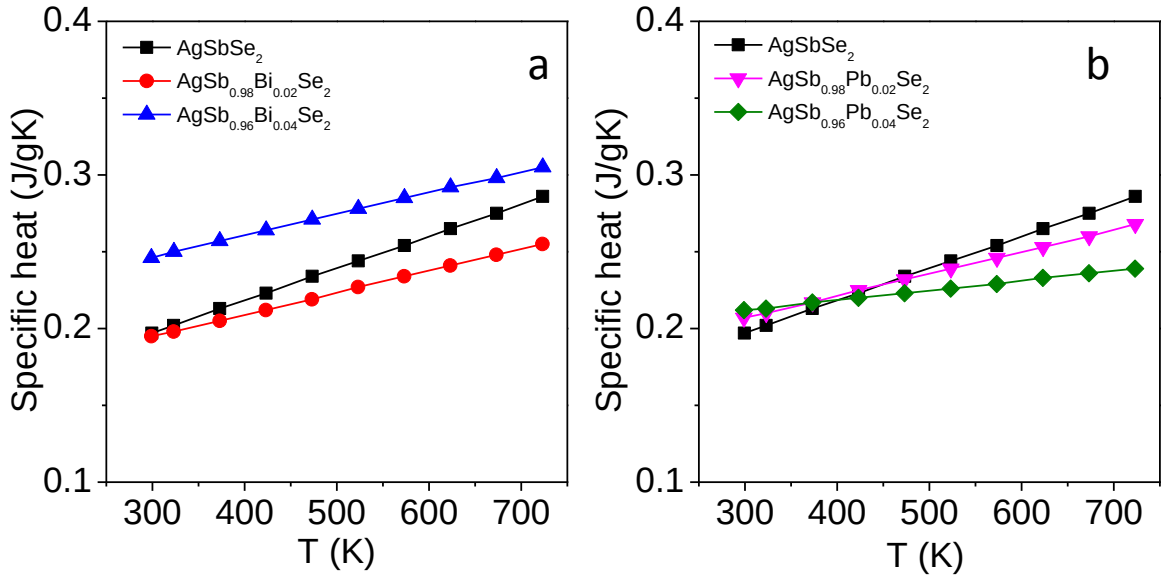

Fig. S3 Temperature dependent specific heat of (a) $AgSb_{1-x}Bi_xSe_2$ (x= 0-0.04) and (b) $AgSb_{1-x}Pb_xSe_2$ (x= 0- 0.04) .

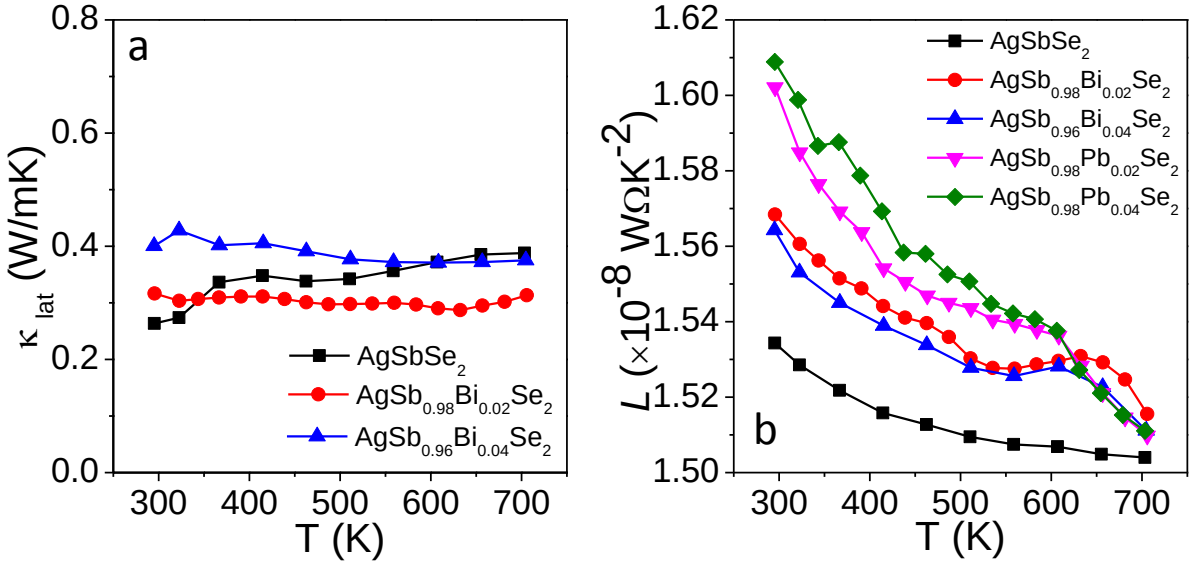

Fig. S4 (a) Temperature dependent lattice thermal conductivity (κ_{lat}) of $AgSb_{1-x}Bi_xSe_2$ (x= 0.02, 0.04) and pristine $AgSbSe_2$. (b) Calculated Lorenz numbers based on the fitting of respective Seebeck coefficient values to estimate the reduced chemical for pristine and doped samples.

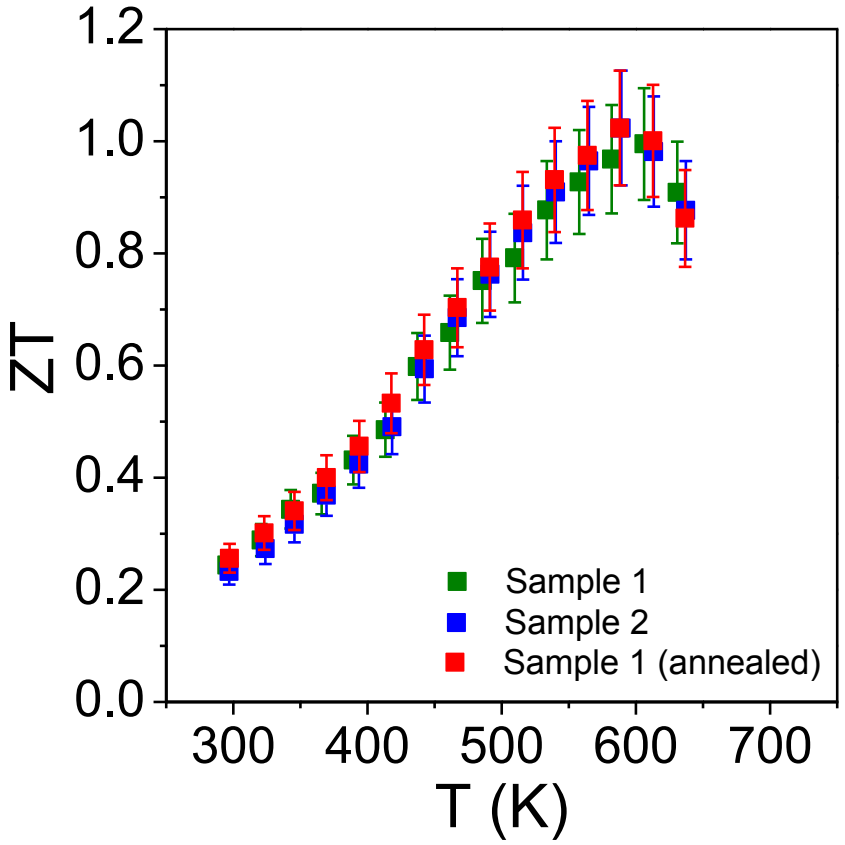

Fig. S5 *ZT* (with 10% error bar) obtained on multiple $AgSb_{0.96}Pb_{0.04}Se_2$ samples with same nominal composition obtained from different synthesis. Annealed (673 K for 15 h) samples also show similar ZT , which confirms the thermal stability at high temperature.

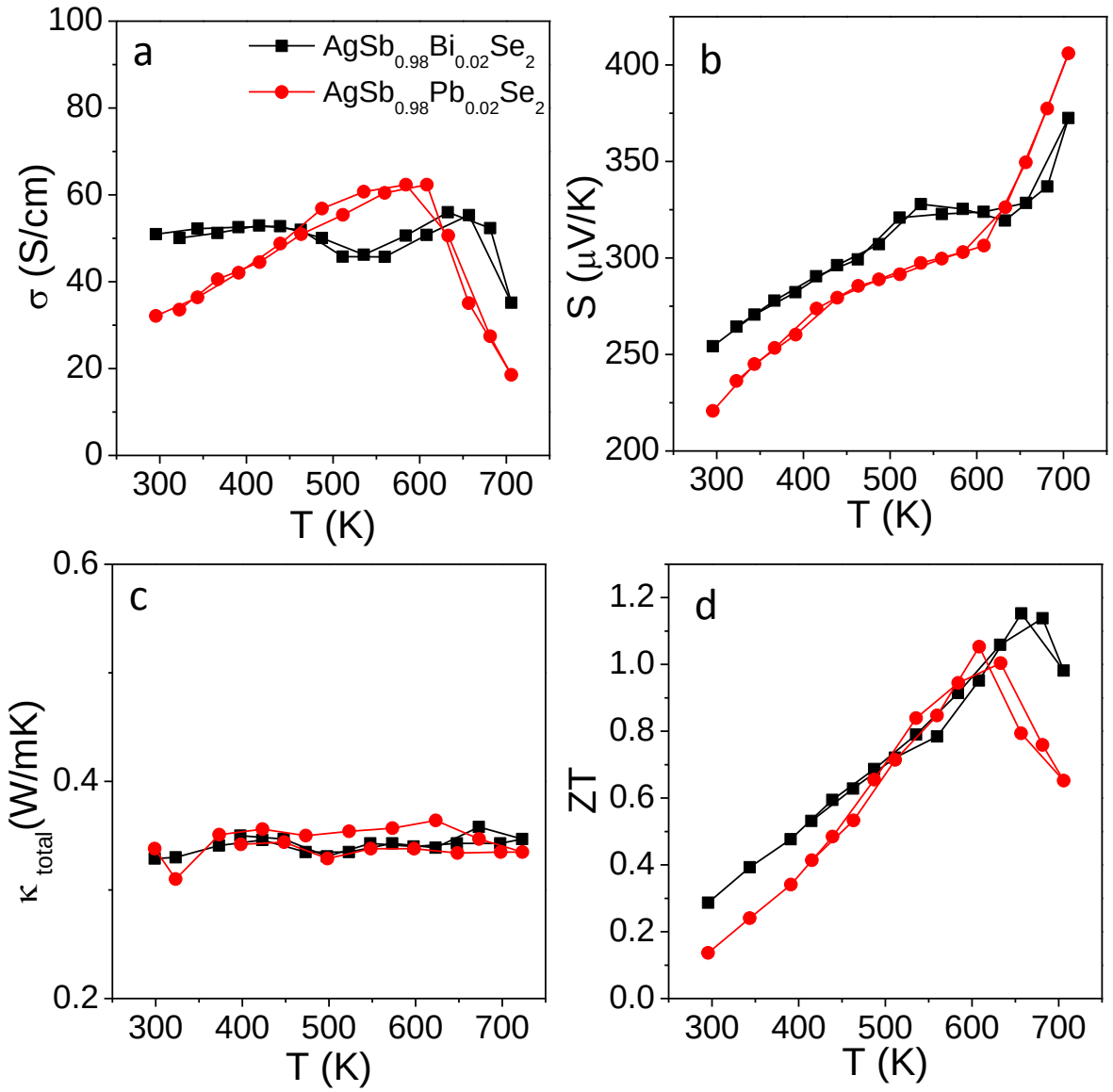

Fig. S6 Heating-cooling cycle of temperature-dependent (a) electrical conductivity (σ), (b) Seebeck coefficient (S), (c) total thermal conductivity (κ_{total}) and (d) thermoelectric figure of merit (ZT) plot of $AgSb_{0.98}Bi_{0.02}Se_2$ and $AgSb_{0.98}Pb_{0.02}Se_2$. Heating and cooling cycles give repeatable transport properties for a given sample, which confirms the high temperature stability of the samples.